Molecular determinants of the aggregation behavior of α- and β-synuclein

ROBERT C. RIVERS,[1] JANET R. KUMITA,[1] GIAN GAETANO TARTAGLIA,[1] MATTHEW M. DEDMON,[1] AMOL PAWAR,[1] MICHELE VENDRUSCOLO,[1] CHRISTOPHER M. DOBSON,[1] AND JOHN CHRISTODOULOU[1–3]

[1]Department of Chemistry, University of Cambridge, Cambridge CB2 1EW, United Kingdom
[2]Institute of Structural Molecular Biology, Research Department of Structural and Molecular Biology, University College London, London WC1E 6BT, United Kingdom
[3]School of Crystallography, Birbeck College, London WC1E 6BT, United Kingdom

(RECEIVED August 16, 2007; FINAL REVISION December 14, 2007; ACCEPTED December 20, 2007)

Abstract

α- and β-synuclein are closely related proteins, the first of which is associated with deposits formed in neurodegenerative conditions such as Parkinson's disease while the second appears to have no relationship to any such disorders. The aggregation behavior of α- and β-synuclein as well as a series of chimeric variants were compared by exploring the structural transitions that occur in the presence of a widely used lipid mimetic, sodium dodecyl sulfate (SDS). We found that the aggregation rates of all these protein variants are significantly enhanced by low concentrations of SDS. In particular, we inserted the 11-residue sequence of mainly hydrophobic residues from the non-amyloid-β-component (NAC) region of α-synuclein into β-synuclein and show that the fibril formation rate of this chimeric protein is only weakly altered from that of β-synuclein. These intrinsic propensities to aggregate are rationalized to a very high degree of accuracy by analysis of the sequences in terms of their associated physicochemical properties. The results begin to reveal that the differences in behavior are primarily associated with a delicate balance between the positions of a range of charged and hydrophobic residues rather than the commonly assumed presence or absence of the highly aggregation-prone region of the NAC region of α-synuclein. This conclusion provides new insights into the role of α-synuclein in disease and into the factors that regulate the balance between solubility and aggregation of a natively unfolded protein.

Keywords: α-synuclein; β-synuclein; aggregation; NMR; protein engineering; fugu

Supplemental material: see www.proteinscience.org

Reprint requests to: John Christodoulou, Institute of Structural Molecular Biology, Research Department of Structural and Molecular Biology, University College London, and School of Crystallography, Birkbeck College, Gower Street, London WC1E 6BT, UK; e-mail: j.christodoulou@ucl.ac.uk; fax: 44-020-7679-7193; or Michele Vendruscolo, Department of Chemistry, University of Cambridge, Lensfield Road, Cambridge CB2 1EW, UK; e-mail:mv245@cam.ac.uk; fax: 44-01223-763418.

Abbreviations: αsyn, α-synuclein; βsyn, β-synuclein; PD, Parkinson's disease; CD, circular dichroism; ThT, ThioflavinT.

Article and publication are at http://www.proteinscience.org/cgi/doi/10.1110/ps.073181508.

Parkinson's disease (PD), the most common neurodegenerative movement disorder, affects an estimated four million individuals worldwide (Moore et al. 2005). PD has been associated with protein misfolding after the discovery that Lewy bodies and Lewy neurites, which are often found deposited in the brains of individuals with PD and the related dementia with Lewy bodies (DLB), are made of abnormal assemblies of α-synuclein (αsyn) (Spillantini et al. 1997, 1998; Baba et al. 1998). It has also been recognized that gene triplication and missense

mutations in αsyn lead to rare familial forms of PD and DLB, thus reinforcing the notion of a causative link between the aggregation of this protein and these diseases (Polymeropoulos et al. 1997; Kruger et al. 1998; Singleton et al. 2003; Chartier-Harlin et al. 2004; Ibanez et al. 2004; Zarranz et al. 2004).

αsyn is one of a small family of intrinsically disordered proteins (~127–140 residues) that includes β-synuclein (βsyn) and γ-synuclein (Jakes et al. 1994; Uversky et al. 2002). The sequence identity (Fig. 1) between αsyn and βsyn is 62% and is highest in the N-terminal region. A considerable sequence divergence occurs in the C-terminal region, although both have a high content of acidic residues. The most significant variation in the sequences of αsyn and βsyn is within the region encompassing residues 61–95 of αsyn. This region, known as the non-amyloid-β component (NAC), because of its reported presence in amyloid-β deposits purified from Alzheimer's disease brain (Ueda et al. 1993), is considered to be key for the assembly of αsyn into fibrils (Han et al. 1995). Moreover, the absence of an 11 amino acid stretch (Val73–Glu83) from the NAC region in βsyn has generally been assumed to be the reason why αsyn and βsyn have different aggregation propensities in vitro (Biere et al. 2000; Hashimoto et al. 2001; Kahle et al. 2001). When isolated, this 12-residue peptide fragment, Val71–Val82 from the NAC region of αsyn, readily forms amyloid fibrils in vitro (Giasson et al. 2001; Madine et al. 2005).

Although the physiological functions of both αsyn and βsyn are as yet unclear (Cookson 2005), current evidence suggests a role in synaptic vesicle homeostasis (Murphy et al. 2000; Narayanan and Scarlata 2001). This suggestion is supported by the presence of conserved, imperfect, KTKEGV repeats in the N-terminal region of both proteins; such repeats are well-known motifs for interactions with lipid vesicles, and indeed both αsyn and βsyn bind to acidic phospholipids (Clayton and George 1998; Davidson et al. 1998; Bussell Jr. and Eliezer 2003). A lipid-mediated function is supported by the observation

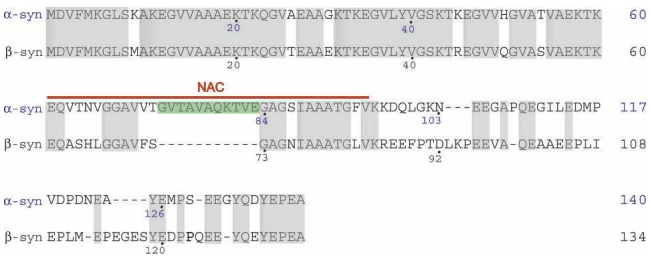

Figure 1. Sequence comparison of human αsyn and βsyn. Sequence gaps have been introduced to optimize similarity. Amino acids highlighted in gray correspond to sequence identity, while the sequence from Gly73 to Glu83 of αsyn highlighted in green indicates the region of αsyn not present in βsyn. The red line indicates the entire NAC region of αsyn.

that both αsyn and βsyn inhibit the production in vitro of phosphatidic acid by the transmembrane protein phospholipase D2 (Payton et al. 2004). The association with lipids confers a high α-helical content to the otherwise disordered protein and appears to be protective toward aggregation (Zhu and Fink 2003).

While many studies have focused on the conformational and aggregation properties of αsyn, there are few similar studies of βsyn. The primary reason for this is probably that βsyn has not been observed to accumulate in Lewy bodies found in the brains of PD victims (Mori et al. 2002). Moreover, unlike αsyn, which readily forms amyloid fibrils in vitro, βsyn appears to remain in a soluble, largely monomeric state even after long periods of incubation (Biere et al. 2000; Uversky et al. 2002; Park and Lansbury Jr. 2003) although aggregates have been formed in vitro under harsh conditions in the presence of high concentrations of lead and zinc (Yamin et al. 2005).

To mimic the nature of interactions that synucleins have with membranes and lipids, micelles of the detergent sodium dodecyl sulfate (SDS) are often used as a standard model for at least some of the features of a lipid environment for polypeptides. The SDS micelle-bound state of αsyn has been well studied (Eliezer et al. 2001; Chandra et al. 2003) since SDS micelles have a molecular weight distribution that is suitable for NMR studies (Eliezer et al. 2001; Chandra et al. 2003). The secondary structure and backbone dynamics of βsyn are very similar to those of αsyn in the SDS micelle-bound state (Sung and Eliezer 2006), suggesting that both proteins interact in a similar manner with membrane mimetics.

Here we describe studies designed to explore further the differences in behavior between αsyn and βsyn. We characterize the structural transitions that occur from the disordered ''native'' state to the α-helical conformation that occurs in the presence of the lipid mimetic SDS and show that βsyn, in a manner similar to αsyn, forms well-ordered amyloid fibrils under mild conditions in the presence of SDS. SDS addition has previously been found to induce fibril formation of a peptide fragment of a complement receptor (Pertinhez et al. 2002), to promote fibril formation in αsyn (Necula et al. 2003; Ahmad et al. 2006), and to lead to the extension of fibrils in β2-microglobulin (Yamamoto et al. 2004).

Increasing evidence suggests that limited portions of the sequences of amyloidogenic proteins play a key role in the aggregation process and take part in the formation of the β-core of the resulting fibrils (Ventura et al. 2004; Esteras-Chopo et al. 2005; Bemporad et al. 2006). We investigate this issue here by comparing the aggregation propensities of αsyn and βsyn, in the presence of SDS. To gain further insight into the sequence determinants of the aggregation of synuclein molecules and to explore the effects on the aggregation properties and the conformational state of

the hydrophobic core of the NAC region found only in αsyn, we used engineered chimeras of αsyn and βsyn (Zibaee et al. 2007) and the synuclein-like proteins from the puffer fish, *Fugu* (Yoshida et al. 2006). This analysis reveals that specific physicochemical differences, in particular in the distribution of electrostatic charges, are crucial in determining the lowered propensity for aggregation of βsyn relative to αsyn, at least under the conditions used in this study, and hence are likely to be the origin of the absence of βsyn in Lewy bodies and other aggregates associated with PD.

Results

SDS induces helical secondary structure in αsyn and βsyn

Several observations relating to αsyn and βsyn, including their ability to inhibit phospholipaseD2 (Jenco et al. 1998) and to associate with synaptic vesicles (Kahle et al. 2002), suggest that their interaction with lipids is an important part of their cellular function. We have therefore probed the structural transitions of these proteins that occur as a result of their transfer from conditions mimicking the native cytosolic state to those resembling a membrane-bound state. For the former we studied the proteins in aqueous solution, and for the latter we used the lipid mimetic SDS (Eliezer et al. 2001; Chandra et al. 2003). Far-UV CD analysis showed that in the absence of SDS and at SDS concentrations below 0.25 mM and using αsyn or βsyn concentrations of 17 μM, the value of $[\Theta]_{222nm}$ is -2800 deg · cm^2 · dmol^{-1}, indicating a low α-helical secondary structure content for both αsyn and βsyn (Fig. 2). As the SDS concentration is increased, the observed helical character of the CD spectra increases. With 40 mM SDS or greater, however, αsyn has a more negative value of $[\Theta]_{222nm}$ than does βsyn, which suggests that αsyn has a higher degree of helical secondary structure than βsyn. To ascertain the full helical potential of these polypeptides we explored the effects of high concentrations of trifluorethanol (TFE) (Lehrman et al. 1990). When the values of $[\Theta]_{222nm}$ in the presence of 40 mM SDS are compared to those found in the presence of 50% TFE, αsyn is found to exhibit >94% of its maximum extent of helicity (Jackson et al. 1991; Kumita et al. 2000) when in the presence of 40 mM SDS while βsyn has only 73%.

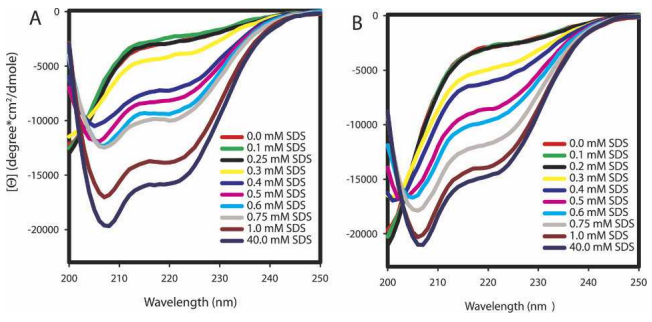

Figure 2. Far-UV CD spectra of (*A*) αsyn and (*B*) βsyn. The spectra were recorded for 17 μM protein, in 10 mM phosphate buffer, 100 mM NaCl at 37°C, pH 7.7 and show a distinct transition from a random to an α-helical conformation in each case as a function of increasing concentrations of SDS.

In the absence of protein, the critical micelle concentration (CMC) of SDS was found to be 0.70 ± 0.05 mM, a value that at first sight suggests that the results described in the outline above were obtained under conditions below the CMC. Studies have shown, however, that the presence of αsyn can reduce substantially the CMC of SDS and other lipid mimics (Necula et al. 2003). In the presence of 15 μM αsyn, the CMC was reduced to 0.09 mM, under slightly differing conditions (Necula et al. 2003), while in the presence of βsyn (15 μM) we found that this value was even further reduced to 0.06 ± 0.02 mM. Consistent with this value for the CMC of both proteins, our CD analysis (Fig. 2) shows that above this concentration of SDS, the α-helical signal (222 nm) gradually increases, indicative of the interaction of the proteins with micellar SDS.

NMR characterization of the SDS-induced helical transition in αsyn and βsyn

We used NMR spectroscopy to compare further the behavior of αsyn and βsyn as the concentration of SDS is increased. The [^{1}H-^{15}N] Heteronuclear Single Quantum Coherence (HSQC) spectrum of βsyn (150 μM) in the absence of SDS and at 10°C (Fig. 3A) shows visible cross-peaks for each non-proline amide group and displays the limited dispersion in the amide proton dimension typical of unfolded proteins (Glushka et al. 1989). We carried out low temperature NMR studies of the native form of the synucleins because the spectra of the N-terminal regions of these proteins are broadened at higher temperatures through intermediate exchange (Eliezer et al. 2001). Also, as was observed previously (Eliezer et al. 2001), the Cα chemical shifts reveal two regions of the sequence (residues 10–26 and 32–69) that have consecutive positive deviations from random-coil values indicative of at least transient α-helical secondary structure; the latter corresponds well with the CD data suggestive of a helical content of ~14% in the unfolded state, while the C-terminal region is more disordered (Fig. 3B).

The Cα chemical shifts of βsyn in the saturated SDS-bound form (40 mM SDS, 40°C, Fig. 4A,B) reveal that SDS induces a significant degree of α-helical structure in the entire N-terminal region (residues 1–83), while the resonances of residues in the C-terminal region (84–134) remain largely unperturbed. These data are similar to

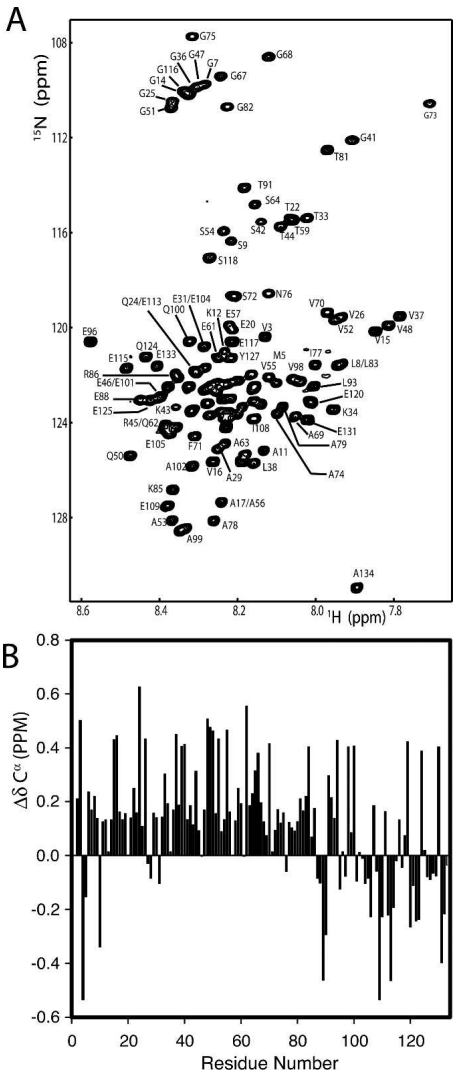

Figure 3. NMR of βsyn in its natively unfolded state. (*A*) [^{1}H-^{15}N] HSQC spectrum of βsyn in 10 mM phosphate buffer, in 100 mM NaCl at 10°C, pH 7.4. (*B*) Deviation of Cα chemical shifts from random-coil values for wild-type βsyn.

αsyn, and the N-terminal region under these conditions forms, in each protein, two contiguous α-helical regions separated by Lys43/Thr44 (Fig. 4B,C; Chandra et al. 2003). In the micelle-bound state, however, the average deviation from random-coil shifts for helix 2 in βsyn is 2.1 ± 0.1 ppm while for helix 2 in αsyn it is 2.6 ± 0.1 ppm. This result suggests that helix 2 is more completely formed in the SDS micelle-bound state of αsyn than it is in βsyn, a result consistent with the CD data discussed above.

To explore further the SDS-induced structural transition from the natively unfolded to the helical states of both αsyn and βsyn, we monitored the chemical shift transitions of backbone $^{1}H^{N}$ and ^{15}N nuclei over increasing concentrations of SDS: Synucleins ratios ranging from 0 to over 250 (corresponding to 0–40 mM SDS with 150 μM protein). At low molar ratios of SDS to protein (2–10 SDS:1 βsyn), we observed the complete broadening of resonances of residues in the N-terminal regions (1–98 and 1–83 in αsyn [Ulmer et al. 2005] and βsyn, respectively), while those of the C-terminal regions remained largely unchanged from those observed in the absence of SDS (Supplemental material). The line broadening of the N-terminal resonances of both proteins could arise from chemical exchange processes, for example between the free or micelle-bound states with rates of exchange that are intermediate on the NMR timescale (milliseconds). CPMG-enhanced HSQC experiments were, however, not able to refocus the chemical shifts from the broadened resonances, a result likely to reflect both the magnitude and heterogeneity of the fluctuations (Mulder et al. 1996).

Fibril formation by αsyn and βsyn at low concentrations of SDS

It has been observed previously that αsyn aggregates in a nucleation-dependent manner under a range of conditions, while βsyn remains in a soluble monomeric form even after long periods of incubation (Biere et al. 2000). However, when the SDS concentration was varied in the experiments described above, we observed that both αsyn and βsyn aggregated after incubation for just a few hours in the range of 0.25–0.75 mM SDS. The aggregates of both proteins formed under these conditions were observed to bind ThioflavinT (ThT) (Fig. 5), and also showed the blue-green birefringence typical of amyloid fibrils with Congo red. EM analysis showed these aggregates to have fibrillar morphology, with protofilament structures and a twist with a periodicity of 35–40-nm segments (Fig. 5B), characteristics typical of amyloid fibrils (Chiti et al. 1999).

We then explored the aggregation behavior of the two proteins in a systematic manner by incubating αsyn and βsyn (70 μM, phosphate buffer, pH 7.7, at 37°C) at varying SDS concentrations from 0 to 5 mM and in each case monitoring the reaction using the enhancement of ThT fluorescence and checking for the presence of fibrils using EM. Fibril formation was highly reproducible for both αsyn and βsyn with agitation of the sample and SDS concentrations ranging from 0 to 0.75 mM for αsyn and 0.25 to 0.75 mM of SDS for βsyn (Fig. 5C,D). That the presence of SDS significantly accelerates the rate of fibril formation is clearly seen with αsyn, where the half-time for aggregation ($t_{1/2}$) is reduced from ~20 h to 4 h (±1 h) in the presence of 0.5 mM SDS (molar ratio 7.1 SDS:1 αsyn). Indeed the overall aggregation rates for both αsyn and βsyn are fastest under the latter conditions that, in fact, correspond to the midpoint of the structural transition

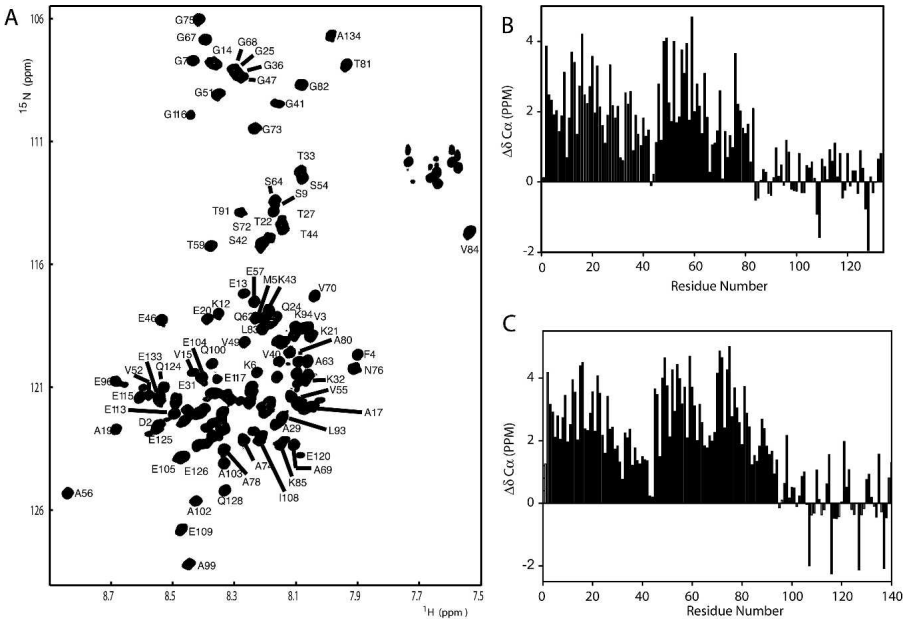

Figure 4. NMR of micelle-bound αsyn and βsyn. (*A*) [^{1}H-^{15}N] HSQC spectrum of βsyn in 10 mM phosphate buffer, 100 mM NaCl, 40 mM SDS, at 40°C, pH 7.4. (*B*) Cα chemical shifts deviations from random-coil values for wild-type βsyn in the presence of 40 mM SDS (40°C). (*C*) Cα chemical shift deviations for micelle bound for αsyn (50 mM SDS, 25°C, taken from Chandra et al. [2003]).

from random-coil to α-helical structure (Fig. 5C,D). Using pulsed-field gradient diffusion NMR, we found that the hydrodynamic radius (22.4 ± 1.6 Å) of SDS at a concentration of 0.1 mM in the presence of 70 μM βsyn (10 mM phosphate buffer, 100 mM NaCl, pH 7.7, 37°C) was closely similar to that expected for a fully formed SDS micelle (~23 Å) (Chandra et al. 2003) composed of 70 molecules of SDS, suggesting that SDS is in a micellar state under the fibril forming conditions, consistent with the reduction of the CMC of SDS in the presence of synuclein.

The formation of fibrils by αsyn and βsyn at low concentrations of SDS in some cases appeared to exhibit biphasic kinetics in which there is an initial increase in ThT fluorescence prior to the exponential growth of fibrillar species. The initial ''burst'' phases do not correspond with the detectable presence of fibrillar material in EM and only slightly (<15%) alter the measured half-lives of the aggregation process $t_{1/2}$. Indeed, EM analysis of samples collected during the lag phase of aggregation indicates the presence of a variety of amorphous aggregates and an occasional appearance of a well-defined fibrillar species. In samples examined during the exponential growth phase, however, EM analysis reveals a host of twisted fibrils with a regular morphology.

Insertion of the NAC region into βsyn and its deletion from αsyn

It is commonly assumed that the absence in βsyn of the 11-residue (Val73–Glu83, Fig. 1) segment within the core of the NAC region of αsyn is a major reason determining the inability of βsyn to form fibrils in vivo (Biere et al. 2000; Giasson et al. 2001). Additionally, it has been reported that removal of residues Val71–Val82 completely abolishes the ability of αsyn to form fibrils (Giasson et al. 2001) under conditions where native αsyn readily does so. To explore the effect of this largely hydrophobic region on the aggregation behavior of βsyn, we prepared and studied a derivative, denoted β+HC, in which residues Val73–Glu83 of αsyn were inserted into the sequence of βsyn following residue 72, as the sequences of the two proteins are aligned up to this residue (Fig. 1). We also prepared two deletion mutants of αsyn in which residues in the NAC region were absent. The first of these mutants is the variant described above (Giasson et al. 2001) (residues Val71–Val82 removed, denoted here as αΔ[71–82]), and the second involves the deletion of residues 73–83, and is denoted αΔ(73–83) (see Supplemental Fig. 2).

Contrary to our initial expectations, β+HC did not form detectable quantities of fibrils in aqueous solution in the absence of SDS under conditions where αsyn does so readily. Incubation and agitation of β+HC with low concentrations of SDS did, however, lead to fibril formation with kinetics very similar to those of βsyn under these conditions, i.e., much slower than αsyn. The half-lives, $t_{1/2}$, of the aggregation reactions were monitored as defined in Materials and Methods, and in each case, an SDS concentration of 0.5 mM was found to lead to the most rapid aggregation for the SDS concentrations

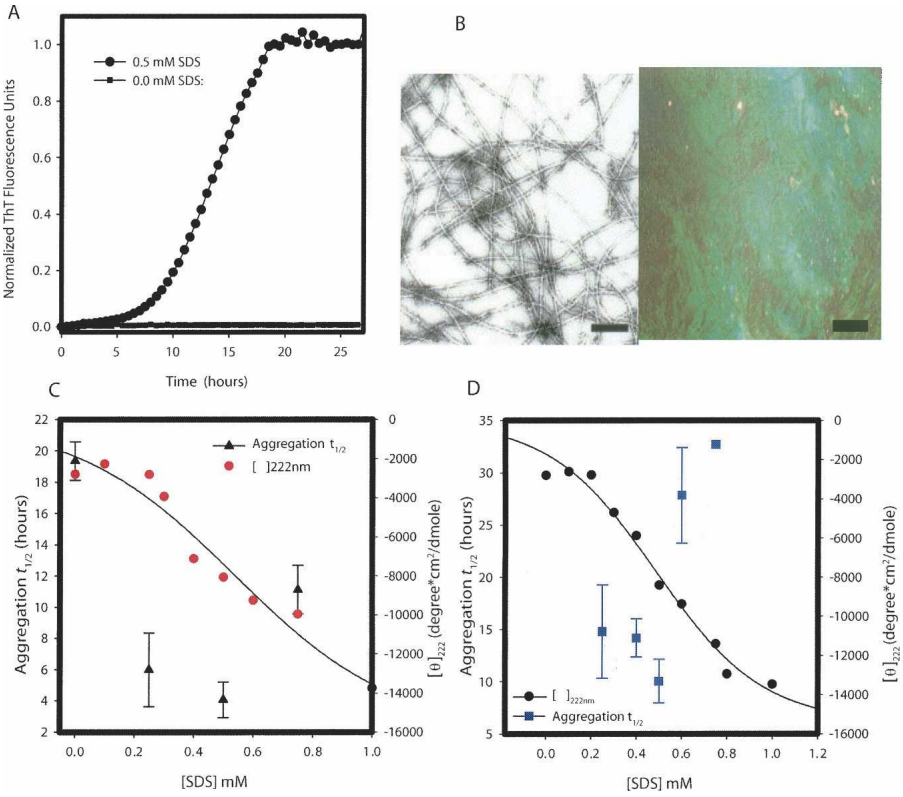

Figure 5. Fibril formation of βsyn. (*A*) Representative example of the fibril formation kinetics of βsyn. An initial increase in ThT fluorescence intensity was sometimes observed prior to a lag phase before an exponential phase of fibril formation and growth; this behavior did not alter significantly the $t_{1/2}$ value for fibril formation or the observed morphology. (*B*) Electron (scale bar 100 nm) and optical (stained with Congo red, scale bar 100 μm) microscopy images of typical βsyn fibrils formed in 0.5mM SDS; the relationship between $t_{1/2}$ for the aggregation reaction and the SDS concentration is overlaid with a plot of θ_{222} as a function of SDS concentration for (*C*) αsyn and (*D*) βsyn. The fastest aggregation rates correspond approximately to the midpoint of the transition from disordered to α-helical secondary structure for both αsyn and βsyn.

explored (0–1 mM) (Supplemental Fig. 3). We then examined the behavior of the two deletion mutants of αsyn under these conditions for comparison with the insertion experiment with βsyn. As with βsyn, the SDS conditions stimulated fibril formation in αΔ(71–82), which has previously been shown not to aggregate detectably in aqueous solution where full-length αsyn readily forms fibrils (Giasson et al. 2001). Intriguingly, the αΔ(73–83) variant also formed fibrils, as was recently shown (Zibaee et al. 2007); interestingly, in the presence of SDS the aggregation rate was faster than that of αsyn under similar conditions despite the absence of the major part of the NAC region (Fig. 6A). The morphologies of fibrillar structures differed somewhat between αΔ(71–82) and αΔ(73–83), with αΔ(71–82) forming fibrils similar to those formed by αsyn, βsyn, and β+HC under the SDS conditions, while the fibrils formed under the same conditions for αΔ(73–83) are less well defined and show less regularity (Fig. 6B).

Rationalization of the observed aggregation rates for the various synucleins

To predict the relative aggregation propensities of the various proteins studied here, we used the Zyggregator algorithm (Pawar et al. 2005), in which the physicochemical properties of sequences of amino acids (hydrophobicity, charge, secondary structure propensity, and pattern of hydrophobic and hydrophilic residues) are used. In this approach, an ''aggregation propensity profile'' (Z_{agg}^{prof}) (Pawar et al. 2005) and an overall intrinsic aggregation propensity score (Z_{agg}) (DuBay et al. 2004) were computed from empirical functions relating the propensities of given polypeptide chains to aggregate compared with a randomly generated set of sequences of amino acids of the same lengths. The Z_{agg}^{prof} profile defines the contribution to the total propensity to aggregate of the different regions along a polypeptide sequence, hence highlighting aggregation-prone and aggregation-sensitive regions (i.e.,

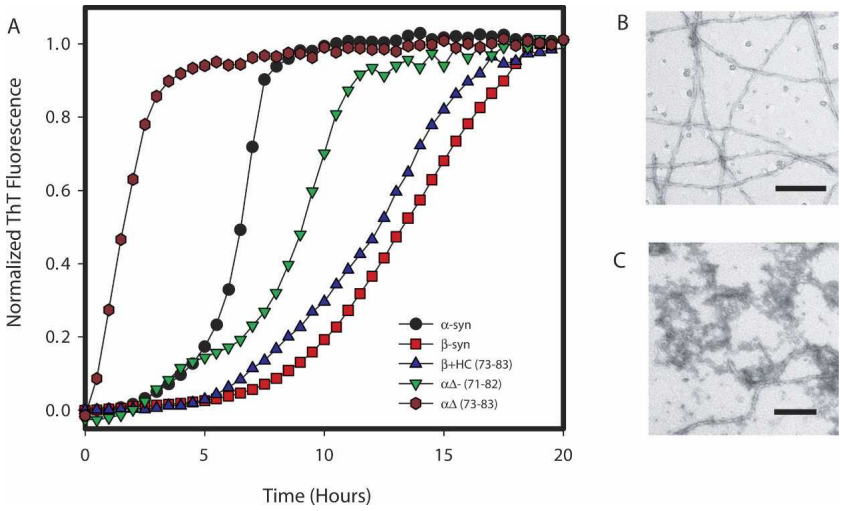

Figure 6. Comparison of fibril formation of synuclein variants. (*A*) Representative example of the kinetics of fibril formation for αsyn, βsyn, β+HC, αΔ(71–82), and αΔ(73–83) (labeled in figure) in 0.5 mM SDS (pH 7.7), 10 mM phosphate buffer, and 100 mM NaCl at 37°C. (*B*) Electron microscopy (scale bar 200 nm) of fibrils formed by αΔ(71–82) in SDS showing fibrils of a twisted morphology similar to those formed by α-syn, βsyn, and β+HC under the same conditions (Fig. 3). (*C*) Electron microscopy images (scale bar 200 nm) of fibrils formed by αΔ(73–83) in SDS conditions show a mixture of fibrils and amorphous aggregates.

where mutations are predicted to have large effects on the aggregation rates). In addition, the Z_{agg} score enables prediction of the relative aggregation rates of different polypeptides under given conditions. If $Z_{agg} > 0$, the sequence is more prone to aggregation than a randomly generated sequence, while it is less prone if $Z_{agg} < 0$.

The comparison of the aggregation propensity profiles of αsyn and βsyn are shown in Figure 7A. Interestingly, the HC region (Val71–Val83), in the context of the αsyn sequence, is not predicted to be highly aggregation prone, despite its high hydrophobic content. The calculated Z_{agg} scores for the synuclein variants studied in this work are reported in Table 1 and compared with the corresponding half-times for aggregation measured in the present study in solutions containing SDS. These variants include synucleins from *Fugu rubripes* (sequences are given in

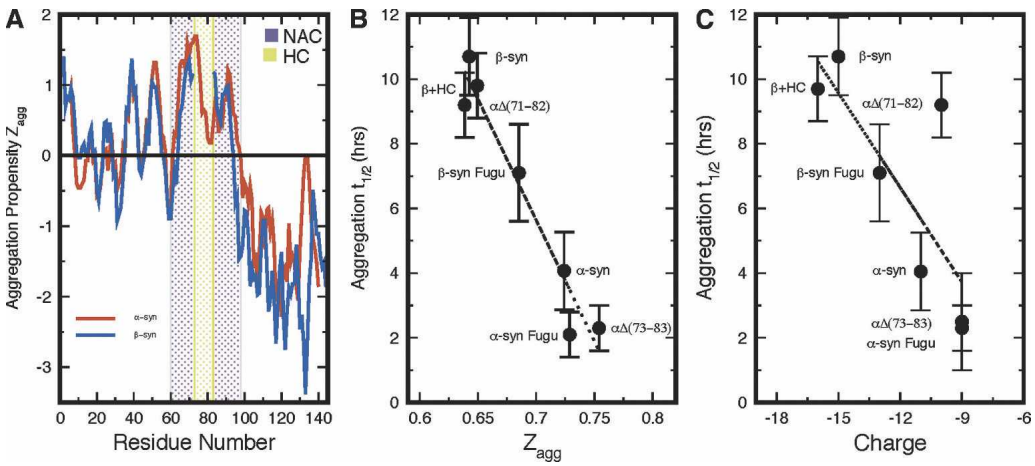

Figure 7. Comparison of observed aggregation rates with predicted aggregation propensities. (*A*) Aggregation propensity profile of αsyn (red) and βsyn (blue) at pH 7.7 with gaps introduced to represent the missing residues (Val73–Glu83) in βsyn. A line at $Z_{agg}^{prof} = 0$ is drawn to identify the aggregation-promoting regions of each sequence that fall *above* this line. Additionally, the region corresponding to the highly amyloidogenic NAC region of αsyn is highlighted in light blue. (*B*) Aggregation $t_{1/2}$ values for αsyn, βsyn, β+HC, αΔ(71–82), αΔ(73–83), *Fugu rubripes* αsyn, and *Fugu rubripes* βsyn plotted relative to the corresponding Z_{agg} scores. The correlation coefficient, 0.96, reflects the excellent agreement between the predictions and the experimental data. (*C*) Plot of the variation of the observed $t_{1/2}$ for the aggregation reactions of the synuclein variants studied here with the overall net charge; the plot shows that the charge interactions are strongly correlated with the observed aggregation rates of the synuclein derivatives under fibril forming conditions (0.5 mM SDS at pH 7.7, 10 mM phosphate, 100 mM NaCl at 37°C).

Table 1. *Aggregation of αsyn, βsyn, and their mutational variants*

Protein	Z_{agg}[a]	k_{app} (h^{-1})[b]	$t_{1/2}$ (h)[b]	Lag time (h)[b]	Charge[c]
αsyn	0.724	1.08 ± 0.16	4.1 ± 0.5	1.9	−11
βsyn	0.643	0.77 ± 0.09	10.7 ± 1.0	9.2	−15
α-Fugu	0.729	2.38 ± 0.30	2.3 ± 0.1	≤0.05	−9
β-Fugu	0.685	0.60 ± 0.05	7.1 ± 0.7	5.9	−13
β+HC	0.639	0.73 ± 0.15	9.8 ± 1.0	8.3	−16
αΔ(73–83)	0.754	2.52 ± 0.46	2.1 ± 0.2	≤0.05	−9
αΔ(71–82)	0.649	0.68 ± 0.16	9.2 ± 0.8	7.6	−10

Solutions contained 70 μM protein, pH 7.7, in 10 mM phosphate buffer, 100 mM NaCl, and 0.5 mM SDS.
[a] Calculated using Zyaggregator (Pawar et al. 2005).
[b] Measured using ThT fluorescence.
[c] Net charges at pH 7.7 estimated from the sequence.

Supplemental Fig. 4) with both *Fugu* αsyn and βsyn sharing ~58% identity with the human proteins. A plot of the observed $t_{1/2}$ values against the calculated Z_{agg} has a correlation coefficient of 0.96 (Fig. 7B). The remarkably high level of this correlation strengthens further the idea that propensities to aggregate are closely linked to the physicochemical properties of a peptide or a protein sequence, even in environments (e.g., SDS at pH 7) that differ significantly from those under which the data used in the derivation of the algorithm (aqueous solution at low pH) were obtained (DuBay et al. 2004; Pawar et al. 2005).

In order to clarify further the role of charged residues in the aggregation process, we calculated a correlation coefficient of 0.79 between the aggregation $t_{1/2}$ values and the overall net charge of the proteins (Fig. 7C). The overall electrostatic charge is one of the factors included in the algorithm used here, and thus the high correlation evident in Figure 7C suggests that the variations in the net charge of the various proteins including the deletion and insertion variants is a major factor in the differences in aggregation rate in this instance. The present study, however, strongly indicates that it is not just the total electrostatic charge that determines the aggregation rates, but the precise location of charged side chains along the sequence.

Discussion

We have shown that both αsyn and βsyn can readily self-assemble into highly ordered amyloid fibrils in vitro in the presence of low concentrations of SDS. Analysis of CD and NMR data confirms that both proteins lack well-defined secondary and tertiary structure in their natively disordered state but acquire α-helical secondary structure in the presence of high concentrations of SDS. When bound to SDS micelles, the N-terminal regions of both proteins (1–100 in αsyn and 1–83 in βsyn) adopt helical structure while the C-terminal region remains highly disordered. The first (N-terminal) helix (residues Met1–Lys43) is similar in the two proteins, as revealed from chemical shift changes, a conclusion in agreement with previously published work (Sung and Eliezer 2006). The second helix, however, is longer in αsyn than that in βsyn, and its chemical shifts deviate more strongly from random-coil values, again in accord with earlier studies (Sung and Eliezer 2006).

There are substantial differences in the affinities of αsyn with different phospholipids (Davidson et al. 1998). These variations are likely to modulate the dynamic exchange processes between the synuclein molecules bound to a membrane surface and those that are free in solution. Within such a dynamical system, specific types of membrane surface could serve to nucleate amyloid formation. Our findings suggest strongly that such membrane interactions could play a potentially crucial role in the aggregation process. In support of this argument, aggregation of αsyn was enhanced in the brain membrane fractions in cell-free experiments (Lee et al. 2002), and additionally, the prion protein also forms amyloid fibrils on the surface of lipid bilayers (Luhrs et al. 2006). In combination with evidence that prefibrillar αsyn oligomers can permeabilize vesicles (Park and Lansbury Jr. 2003), these findings underscore the necessity of understanding in detail the membrane/lipid-bound state of the synuclein molecules.

The results described in this article show that the increase in the propensities of both αsyn and βsyn to form amyloid fibrils begins to decline at approximately the midpoint of the transition from the unfolded to the micelle-bound proteins induced by SDS. In light of this observation, we suggest that the enhanced rates of fibril formation by the synucleins in the presence of low concentrations of SDS are associated with an increase in the local concentration of protein molecules at the surface of SDS micelles (Necula et al. 2003). Thus, at low SDS concentrations, where these rate enhancements occur, the number of protein molecules exceeds the number of micelles, giving rise to multiple protein molecules being bound to each micelle. The increased population of aggregation-prone conformations under these low SDS conditions can be inferred from the observed increase in the surface exposure of hydrophobic groups in αsyn (Ahmad et al. 2006). At higher SDS:protein ratios, by contrast, the number of micelles increases to a level where there are more micelles than protein molecules; the latter are therefore efficiently sequestered and isolated in individual micelles. Moreover, the high degree of helicity induced at higher SDS concentrations reflects the increased strength of intramolecular interactions, reducing

the propensity of the protein molecules to form the intermolecular interactions that are the hallmark of amyloid formation.

We have shown in the present study that, contrary to previous evidence, βsyn is able to form fibrils readily under conditions that are physiologically relevant. While previous studies implicated the stretches of primarily hydrophobic residues in the N-terminal region of αsyn, Val66–Val74 (Du et al. 2003) and Val71–Val82 (Giasson et al. 2001), as being key determinants of fibril formation, we showed that the chimeric protein β+HC, which comprises all these regions, does not share the rapid aggregation properties of αsyn and does not form fibrils in aqueous solution in the absence of aggregation inducers. Indeed we have shown that in terms of fibril formation, β+HC is remarkably similar to βsyn despite the addition of a series of hydrophobic residues. This result shows that it is essential to consider fibril formation in the context of an intact protein sequence, rather than by studying a series of short peptide fragments corresponding to specific regions of the protein, valuable as the latter can be in many other respects (Zurdo 2005).

The differences in the behavior of the two variants of αsyn (αΔ[71–82] and αΔ[73–83]) containing only portions of the NAC region have shed new light on the role of the NAC region itself in the aggregation of αsyn. In stark contrast to the relatively small changes in the aggregation rate of βsyn upon the incorporation of these 11 residues, Val71–Val82, there is considerable variation in the relative aggregation propensity of αsyn through deletions of residues Val71–Val82 (αΔ[71–82]) and Gly73–Glu83 (αΔ[73–83]) even though the deleted regions may appear to be closely similar. Our predictions suggest that the decreased half-time ($t_{1/2}$) for aggregation of αΔ(73–83) found under these conditions results primarily from the removal of a single charged group (Glu83). The incorporation of charged residues into this region of αsyn has previously been shown to depress the rate of fibril formation because of the inhibiting effects of charge on protein–protein interactions and suggests a possible role of Glu83 as a gatekeeper residue to reduce the aggregation propensity (Giasson et al. 2001). The idea that regulatory residues are strategically positioned within core regions of proteins to play critical roles in both folding (Vendruscolo et al. 2001) and aggregation has been shown in the case of the S6 protein (Otzen et al. 2000). By contrast we measured a greatly increased $t_{1/2}$ value for the αΔ(71–82) variant with respect to both αsyn and the αΔ(73–83) variant. The deletion of the 12-residue fragment Val71–Val82 results in a decrease in the global charge by one unit (from −11 to −10, due to the removal of Lys80), while it maintains the presence of Glu83. Thus, electrostatic effects appear to account only in part for the difference in the aggregation propensity of the αΔ(71–82) variant with respect to αsyn and the αΔ(73–83) variant, and we thus suggest that Val71 and Thr72 contribute significantly to the aggregation propensity of αsyn.

Increasing evidence suggests that the rates of aggregation and the location of aggregation-specific regions of proteins and polypeptides can be interpreted in terms of their physicochemical properties (Chiti et al. 2003; DuBay et al. 2004; Fernandez-Escamilla et al. 2004; Lopez de la Paz and Serrano 2004; Pawar et al. 2005). We have used this approach to rationalize in a quantitative manner the aggregation behavior of the synuclein variants used in this study. The predicted intrinsic aggregation propensities (Z_{agg} scores) of these proteins are remarkably well correlated (correlation coefficient 0.96) with the experimentally observed aggregation kinetics. These Z_{agg} scores were calculated with an algorithm that incorporates hydrophobicity, hydrophobic patterns, secondary structure preferences, and the positions of charged residues as key determinants of aggregation. The predictive ability of this approach, as demonstrated in the present study, suggests that simple physicochemical factors are important in determining the propensities for aggregation of proteins in the synuclein family.

Our results show the importance of considering the intact sequences of proteins in determining their aggregation rates. Approaches based on the analysis of the fibrillogenic propensities of short peptides corresponding to small regions of the protein molecules (Giasson et al. 2001; Madine et al. 2005) suggested the peptide fragment, consisting of residues Val71–Val82 of αsyn, to be the most critical region for accounting for the differences in aggregation behavior of αsyn and βsyn. As we have shown here, however, the insertion of the Val71–Val82 fragment of αsyn into βsyn does not result in an increased tendency to aggregate. Consideration of the whole sequence, however, suggests that a delicate balance between the overall distribution of electrostatic charges and hydrophobic regions of the protein is responsible for the much reduced propensity of βsyn to aggregate compared to αsyn.

The combined in vitro and in silico analysis of the aggregation behavior of αsyn and βsyn presented in this work reveals that strategically positioned electrostatic charges, together with the presence of hydrophobic and highly aggregation-prone regions, constitute the critical factors that determine the behavior of these two closely related proteins. In addition, the finding that interaction with membrane mimetics can have dramatic effects on the aggregation behavior of proteins, either to increase or decrease their propensities to form amyloid fibrils depending on the concentration, indicates the profound significance that the environment can have on the propensity of specific proteins to aggregate in living systems.

Materials and Methods

Protein expression and purification

Human recombinant αsyn and βsyn were expressed in *Escherichia coli* BL21(DE3) cells using plasmid pT7-7 for αsyn or pRK172 plasmid for βsyn and purified as previously described (Hoyer et al. 2002; Uversky et al. 2002). Protein purities were >95% as determined by SDS-PAGE, and molecular masses were confirmed by electrospray mass spectrometry.

Circular dichroism measurements

Far-UV CD measurements were performed on a Jasco J-810 spectropolarimeter typically using a protein concentration of 70 μM at 37°C and 1.0-mm path length cell.

Congo red staining

For Congo red birefringence experiments, aliquots of aggregated protein were air-dried onto glass slides. The resulting films were stained with a saturated solution of Congo red and taken to pH 10.0. The stained slides were examined between cross-polarizers using an optical microscope.

Measurement of the critical micelle concentration

The CMC of SDS in different environments was determined using the fluorescence probe ANS as described previously (Yamamoto et al. 2004).

Electron microscopy

Images were obtained using a Phillips CEM100 transmission electron microscope. Samples were prepared from 10-μL aliquots of the relevant aggregation reaction using negative staining by 2% (w/v) uranyl acetate on Formvar-coated nickel grids.

NMR spectroscopy

Isotopically enriched αsyn and βsyn were expressed in *E. coli* as described above, using M9 minimal medium with 1 g/L $^{15}NH_4Cl$ and 3 g/L ^{13}C-glucose/^{12}C-glucose as the sole nitrogen and carbon sources, respectively. 2D ^{15}N-^{1}H HSQC spectra of solutions containing βsyn were collected on a Bruker Avance 700-MHz spectrometer equipped with a triple-resonance cryogenic probe head. NMR samples of the monomeric free state of syn contained 100 μM protein in 10 mM phosphate, pH 7.4, 100 mM NaCl, with 10% D_2O at 10°C. For samples containing <0.5 mM SDS, spectra were recorded at 10°C while for samples containing >0.5 mM of SDS, an elevated temperature of 40°C was used to collect the spectra. Resonance assignment was performed using standard triple-resonance experiments (Sattler et al. 1999). ^{1}H PG-SLED NMR experiments (Jones et al. 1997) were performed on a solution of SDS with βsyn to determine the hydrodynamic radius of SDS. Dioxan was used as an internal reference compound (Wilkins et al. 1999). NMR data were processed with NMRPipe (Delaglio et al. 1995) and analyzed using Sparky (http://www.cgl.ucsf.edu/home/sparky/).

ThT fluorescence and measurement of aggregation kinetics

Solutions for fluorescence analysis in the presence of ThT contained 70 μM protein in 10 mM phosphate buffer and 100 mM NaCl at pH 7.7, with varying concentrations of SDS. For kinetic aggregation studies, 20 μM ThT (Sigma) was included prior to aggregation. After filtration using 0.22 μm sterile filters, aggregation was induced by heating samples to 37°C with magnetic stirring, with readings taken every 30 min using a Cary Eclipse fluorescence spectrophotometer with excitation at 450 nm, emission at 485 nm, and an averaging time of 10 s. Kinetic traces were normalized to a scale of 0 to 1. Data were processed with SigmaPlot and fitted to a three-parameter sigmoidal equation:

$$y = \frac{a}{1 + e^{\frac{-(x - x_o)}{b}}}$$

where y equals the ThT fluorescence intensity, x is equivalent to time in hours, x_0 is the value of $t_{1/2}$ in hours, and k_{app} is the apparent rate constant for fibril growth and is given by $1/b$ (h^{-1}). The lag time is given again in hours by $x_0 - 2b$.

Prediction of aggregation behavior

An algorithm developed to calculate the intrinsic aggregation propensity (Z_{agg}) of a sequence based on the physicochemical properties of amino acids (DuBay et al. 2004) was used to predict the relative aggregation rates of the different sequences analyzed in this study. Profiles to identify the aggregation behavior of specific regions of the proteins were produced and analyzed by using a modified version of the Zyggregator algorithm (www-vendruscolo.ch.cam.ac.uk/zyggregator.php). The version used in this study includes a treatment of the specific location of charged residues, in order to describe the phenomenon of gatekeeping (G. Tartaglia, A. Pawar, S. Campioni, C. Dobson, F. Chiti, and M. Vendruscolo, unpubl.).

Electronic supplemental information

The file Rivers_SuppInfo.pdf contains four figures, which are referred to in the text and contain additional data and sequence comparisons to support the main article.

Acknowledgments

We thank the Wellcome and Leverhulme Trusts for their support of this research. R.C.R. and A.P. are recipients of studentships from the Gates Cambridge Trust. We also would like to thank Michel Goedert (MRC Laboratory of Molecular Biology, Cambridge) for his generous provision of the synuclein constructs employed in this study and for stimulating and insightful discussions. Additionally, we express our thanks to the staff and acknowledge the use of the Biomolecular NMR Facility, Department of Chemistry, Cambridge.

References

Ahmad, M.F., Ramakrishna, T., Raman, B., and Rao, Ch.M. 2006. Fibrillogenic and non-fibrillogenic ensembles of SDS-bound human α-synuclein. *J. Mol. Biol.* **364:** 1061–1072.

Baba, M., Nakajo, S., Tu, P.H., Tomita, T., Nakaya, K., Lee, V.M., Trojanowski, J.Q., and Iwatsubo, T. 1998. Aggregation of α-synuclein in Lewy bodies of sporadic Parkinson's disease and dementia with Lewy bodies. *Am. J. Pathol.* **152:** 879–884.

Bemporad, F., Calloni, G., Campioni, S., Plakoutsi, G., Taddei, N., and Chiti, F. 2006. Sequence and structural determinants of amyloid fibril formation. *Acc. Chem. Res.* **39:** 620–627.

Biere, A.L., Wood, S.J., Wypych, J., Steavenson, S., Jiang, Y., Anafi, D., Jacobsen, F.W., Jarosinski, M.A., Wu, G.-M., Louis, J.-C., et al. 2000. Parkinson's disease-associated α-synuclein is more fibrillogenic than β- and γ-synuclein and cannot cross-seed its homologs. *J. Biol. Chem.* **275:** 34574–34579.

Bussell Jr., R. and Eliezer, D. 2003. A structural and functional role for 11-mer repeats in α-synuclein and other exchangeable lipid binding proteins. *J. Mol. Biol.* **329:** 763–778.

Chandra, S., Chen, X., Rizo, J., Jahn, R., and Sudhof, T.C. 2003. A broken α-helix in folded α-synuclein. *J. Biol. Chem.* **278:** 15313–15318.

Chartier-Harlin, M.C., Kachergus, J., Roumier, C., Mouroux, V., Douay, X., Lincoln, S., Levecque, C., Larvor, L., Andrieux, J., Hulihan, M., et al. 2004. α-Synuclein locus duplication as a cause of familial Parkinson's disease. *Lancet* **364:** 1167–1169.

Chiti, F., Webster, P., Taddei, N., Clark, A., Stefani, M., Ramponi, G., and Dobson, C.M. 1999. Designing conditions for in vitro formation of amyloid protofilaments and fibrils. *Proc. Natl. Acad. Sci.* **96:** 3590–3594.

Chiti, F., Stefani, M., Taddei, N., Ramponi, G., and Dobson, C.M. 2003. Rationalization of the effects of mutations on peptide and protein aggregation rates. *Nature* **424:** 805–808.

Clayton, D.F. and George, J.M. 1998. The synucleins: A family of proteins involved in synaptic function, plasticity, neurodegeneration and disease. *Trends Neurosci.* **21:** 249–254.

Cookson, M.R. 2005. The biochemistry of Parkinson's disease. *Annu. Rev. Biochem.* **74:** 29–52.

Davidson, W.S., Jonas, A., Clayton, D.F., and George, J.M. 1998. Stabilization of α-synuclein secondary structure upon binding to synthetic membranes. *J. Biol. Chem.* **273:** 9443–9449.

Delaglio, F., Grzesiek, S., Vuister, G.W., Zhu, G., Pfeifer, J., and Bax, A. 1995. NMRPipe: A multidimensional spectral processing system based on UNIX pipes. *J. Biomol. NMR* **6:** 277–293.

Du, H.N., Tang, L., Luo, X.Y., Li, H.T., Hu, J., Zhou, J.W., and Hu, H.Y. 2003. A peptide motif consisting of glycine, alanine, and valine is required for the fibrillization and cytotoxicity of human α-synuclein. *Biochemistry* **42:** 8870–8878.

DuBay, K.F., Pawar, A.P., Chiti, F., Zurdo, J., Dobson, C.M., and Vendruscolo, M. 2004. Prediction of the absolute aggregation rates of amyloidogenic polypeptide chains. *J. Mol. Biol.* **341:** 1317–1326.

Eliezer, D., Kutluay, E., Bussell Jr., R., and Browne, G. 2001. Conformational properties of α-synuclein in its free and lipid-associated states. *J. Mol. Biol.* **307:** 1061–1073.

Esteras-Chopo, A., Serrano, L., and Lopez de la Paz, M. 2005. The amyloid stretch hypothesis: Recruiting proteins toward the dark side. *Proc. Natl. Acad. Sci.* **102:** 16672–16677.

Fernandez-Escamilla, A.M., Rousseau, F., Schymkowitz, J., and Serrano, L. 2004. Prediction of sequence-dependent and mutational effects on the aggregation of peptides and proteins. *Nat. Biotechnol.* **22:** 1302–1306.

Giasson, B.I., Murray, I.V.J., Trojanowski, J.Q., and Lee, V.M.-Y. 2001. A hydrophobic stretch of 12 amino acid residues in the middle of α-synuclein is essential for filament assembly. *J. Biol. Chem.* **276:** 2380–2386.

Glushka, J., Lee, M., Coffin, S., and Cowburn, D. 1989. ^{15}N chemical shifts of backbone amides in bovine pancreatic trypsin inhibitor and apamin. *J. Am. Chem. Soc.* **111:** 7716–7722.

Han, H., Weinreb, P.H., and Lansbury Jr., P.T. 1995. The core Alzheimer's peptide NAC forms amyloid fibrils which seed and are seeded by β-amyloid: Is NAC a common trigger or target in neurodegenerative disease? *Chem. Biol.* **2:** 163–169.

Hashimoto, M., Rockenstein, E., Mante, M., Mallory, M., and Masliah, E. 2001. β-Synuclein inhibits α-synuclein aggregation: A possible role as an Anti-Parkinsonian factor. *Neuron* **32:** 213–223.

Hoyer, W., Antony, T., Cherny, D., Heim, G., Jovin, T.M., and Subramaniam, V. 2002. Dependence of α-synuclein aggregate morphology on solution conditions. *J. Mol. Biol.* **322:** 383–393.

Ibanez, P., Bonnet, A.M., Debarges, B., Lohmann, E., Tison, F., Pollak, P., Agid, Y., Durr, A., and Brice, A. 2004. Causal relation between α-synuclein gene duplication and familial Parkinson's disease. *Lancet* **364:** 1169–1171.

Jackson, D.Y., King, D.S., Chmielewski, J., Singh, S., and Schultz, P.G. 1991. General approach to the synthesis of short α-helical peptides. *J. Am. Chem. Soc.* **113:** 9391–9392.

Jakes, R., Spillantini, M.G., and Goedert, M. 1994. Identification of two distinct synucleins from human brain. *FEBS Lett.* **345:** 27–32.

Jenco, J.M., Rawlingson, A., Daniels, B., and Morris, A.J. 1998. Regulation of phospholipase D2: Selective inhibition of mammalian phospholipase D isoenzymes by α- and β-synucleins. *Biochemistry* **37:** 4901–4909.

Jones, J.A., Wilkins, D.K., Smith, L.J., and Dobson, C.M. 1997. Characterisation of protein unfolding by NMR diffusion measurements. *J. Biomol. NMR* **10:** 199–203.

Kahle, P.J., Neumann, M., Ozmen, L., Muller, V., Odoy, S., Okamoto, N., Jacobsen, H., Iwatsubo, T., Trojanowski, J.Q., Takahashi, H., et al. 2001. Selective insolubility of α-synuclein in human Lewy body diseases is recapitulated in a transgenic mouse model. *Am. J. Pathol.* **159:** 2215–2225.

Kahle, P.J., Haass, C., Kretzschmar, H.A., and Neumann, M. 2002. Structure/function of α-synuclein in health and disease: Rational development of animal models for Parkinson's and related diseases. *J. Neurochem.* **82:** 449–457.

Kruger, R., Kuhn, W., Muller, T., Woitalla, D., Graeber, M., Kosel, S., Przuntek, H., Epplen, J.T., Schols, L., and Riess, O. 1998. Ala30Pro mutation in the gene encoding α-synuclein in Parkinson's disease. *Nat. Genet.* **18:** 106–108.

Kumita, J.R., Smart, O.S., and Woolley, G.A. 2000. Photo-control of helix content in a short peptide. *Proc. Natl. Acad. Sci.* **97:** 3803–3808.

Lee, H.J., Choi, C., and Lee, S.J. 2002. Membrane-bound α-synuclein has a high aggregation propensity and the ability to seed the aggregation of the cytosolic form. *J. Biol. Chem.* **277:** 671–678.

Lehrman, S.R., Tuls, J.L., and Lund, M. 1990. Peptide α-helicity in aqueous trifluoroethanol: Correlations with predicted α-helicity and the secondary structure of the corresponding regions of bovine growth hormone. *Biochemistry* **29:** 5590–5596.

Lopez de la Paz, M. and Serrano, L. 2004. Sequence determinants of amyloid fibril formation. *Proc. Natl. Acad. Sci.* **101:** 87–92.

Luhrs, T., Zahn, R., and Wuthrich, K. 2006. Amyloid formation by recombinant full-length prion proteins in phospholipid bicelle solutions. *J. Mol. Biol.* **357:** 833–841.

Madine, J., Doig, A.J., Kitmitto, A., and Middleton, D.A. 2005. Studies of the aggregation of an amyloidogenic α-synuclein peptide fragment. *Biochem. Soc. Trans.* **33:** 1113–1115.

Moore, D.J., West, A.B., Dawson, V.L., and Dawson, T.M. 2005. Molecular pathophysiology of Parkinson's disease. *Annu. Rev. Neurosci.* **28:** 57–87.

Mori, F., Inenaga, C., Yoshimoto, M., Umezu, H., Tanaka, R., Takahashi, H., and Wakabayashi, K. 2002. α-Synuclein immunoreactivity in normal and neoplastic Schwann cells. *Acta Neuropathol. (Berl.)* **103:** 145–151.

Mulder, F., Spronk, C., Slijper, M., Kapetein, R., and Boelens, R. 1996. Improved HSQC experiments for the observation of exchange broadened signals. *J. Biomol. NMR* **8:** 223–228.

Murphy, D.D., Rueter, S.M., Trojanowski, J.Q., and Lee, V.M.-Y. 2000. Synucleins are developmentally expressed, and α-synuclein regulates the size of the presynaptic vesicular pool in primary hippocampal neurons. *J. Neurosci.* **20:** 3214–3220.

Narayanan, V. and Scarlata, S. 2001. Membrane binding and self-association of α-synucleins. *Biochemistry* **40:** 9927–9934.

Necula, M., Chirita, C.N., and Kuret, J. 2003. Rapid anionic micelle-mediated α-synuclein fibrillization in vitro. *J. Biol. Chem.* **278:** 46674–46680.

Otzen, D.E., Kristensen, O., and Oliveberg, M. 2000. Designed protein tetramer zipped together with a hydrophobic Alzheimer homology: A structural clue to amyloid assembly. *Proc. Natl. Acad. Sci.* **97:** 9907–9912.

Park, J.Y. and Lansbury Jr., P.T. 2003. β-Synuclein inhibits formation of α-synuclein protofibrils: A possible therapeutic strategy against Parkinson's disease. *Biochemistry* **42:** 3696–3700.

Pawar, A.P., Dubay, K.F., Zurdo, J., Chiti, F., Vendruscolo, M., and Dobson, C.M. 2005. Prediction of "aggregation-prone" and "aggregation-susceptible" regions in proteins associated with neurodegenerative diseases. *J. Mol. Biol.* **350:** 379–392.

Payton, J.E., Perrin, R.J., Woods, W.S., and George, J.M. 2004. Structural determinants of PLD2 inhibition by α-synuclein. *J. Mol. Biol.* **337:** 1001–1009.

Pertinhez, T.A., Bouchard, M., Smith, R.A., Dobson, C.M., and Smith, L.J. 2002. Stimulation and inhibition of fibril formation by a peptide in the presence of different concentrations of SDS. *FEBS Lett.* **529:** 193–197.

Polymeropoulos, M.H., Lavedan, C., Leroy, E., Ide, S.E., Dehejia, A., Dutra, A., Pike, B., Root, H., Rubenstein, J., Boyer, R., et al. 1997. Mutation in the α-synuclein gene identified in families with Parkinson's disease. *Science* **276:** 2045–2047.

Sattler, M., Schuleucher, J., and Griesinger, C. 1999. Heteronuclear multidimensional NMR experiments for the structure determination of proteins

in solution employing pulsed field gradients. *Prog. Nucl. Magn. Reson. Spectrosc.* **34:** 93–158.

Singleton, A.B., Farrer, M., Johnson, J., Singleton, A., Hague, S., Kachergus, J., Hulihan, M., Peuralinna, T., Dutra, A., Nussbaum, R., et al. 2003. α-Synuclein locus triplication causes Parkinson's disease. *Science* **302:** 841. doi: 10.1126/science.1090278.

Spillantini, M.G., Schmidt, M.L., Lee, V.M., Trojanowski, J.Q., Jakes, R., and Goedert, M. 1997. α-Synuclein in Lewy bodies. *Nature* **388:** 839–840.

Spillantini, M.G., Crowther, R.A., Jakes, R., Hasegawa, M., and Goedert, M. 1998. α-Synuclein in filamentous inclusions of Lewy bodies from Parkinson's disease and dementia with Lewy bodies. *Proc. Natl. Acad. Sci.* **95:** 6469–6473.

Sung, Y.H. and Eliezer, D. 2006. Secondary structure and dynamics of micelle bound β- and γ-synuclein. *Protein Sci.* **15:** 1162–1174.

Ueda, K., Fukushima, H., Masliah, E., Xia, Y., Iwai, A., Yoshimoto, M., Otero, D., Kondo, J., Ihara, Y., and Saitoh, T. 1993. Molecular cloning of cDNA encoding an unrecognized component of amyloid in Alzheimer disease. *Proc. Natl. Acad. Sci.* **90:** 11282–11286.

Ulmer, T.S., Bax, A., Cole, N.B., and Nussbaum, R.L. 2005. Structure and dynamics of micelle-bound human α-synuclein. *J. Biol. Chem.* **280:** 9595–9603.

Uversky, V.N., Li, J., Souillac, P., Millett, I.S., Doniach, S., Jakes, R., Goedert, M., and Fink, A.L. 2002. Biophysical properties of the synucleins and their propensities to fibrillate. Inhibition of α-synuclein assembly by β- and γ-synucleins. *J. Biol. Chem.* **277:** 11970–11978.

Vendruscolo, M., Paci, E., Dobson, C.M., and Karplus, M. 2001. Three key residues form a critical contact network in a protein folding transition state. *Nature* **409:** 641–645.

Ventura, S., Zurdo, J., Narayanan, S., Parreno, M., Mangues, R., Reif, B., Chiti, F., Giannoni, E., Dobson, C.M., Aviles, F.X., et al. 2004. Short amino acid stretches can mediate amyloid formation in globular proteins: The Src homology 3 (SH3) case. *Proc. Natl. Acad. Sci.* **101:** 7258–7263.

Wilkins, D.K., Grimshaw, S.B., Receveur, V., Dobson, C.M., Jones, J.A., and Smith, L.J. 1999. Hydrodynamic radii of native and denatured proteins measured by pulse field gradient NMR techniques. *Biochemistry* **38:** 16424–16431.

Yamamoto, S., Hasegawa, K., Yamaguchi, I., Tsutsumi, S., Kardos, J., Goto, Y., Gejyo, F., and Naiki, H. 2004. Low concentrations of sodium dodecyl sulfate induce the extension of β_2-microglobulin-related amyloid fibrils at a neutral pH. *Biochemistry* **43:** 11075–11082.

Yamin, G., Munishkina, L.A., Karymov, M.A., Lyubchenko, Y.L., Uversky, V.N., and Fink, A.L. 2005. Forcing non-amyloidogenic β-synuclein to fibrillate. *Biochemistry* **44:** 9096–9107.

Yoshida, H., Craxton, M., Jakes, R., Zibaee, S., Tavare, R., Fraser, G., Serpell, L.C., Davletov, B., Crowther, R.A., and Goedert, M. 2006. Synuclein proteins of the pufferfish *Fugu rubripes*: Sequences and functional characterization. *Biochemistry* **45:** 2599–2607.

Zarranz, J.J., Alegre, J., Gomez-Esteban, J.C., Lezcano, E., Ros, R., Ampuero, I., Vidal, L., Hoenicka, J., Rodriguez, O., Atares, B., et al. 2004. The new mutation, E46K, of α-synuclein causes Parkinson and Lewy body dementia. *Ann. Neurol.* **55:** 164–173.

Zhu, M. and Fink, A.L. 2003. Lipid binding inhibits α-synuclein fibril formation. *J. Biol. Chem.* **278:** 16873–16877.

Zibaee, S., Jakes, R., Fraser, G., Serpell, L.C., Crowther, R.A., and Goedert, M. 2007. Sequence determinants for amyloid fibrillogenesis of human α-synuclein. *J. Mol. Biol.* **374:** 454–464.

Zurdo, J. 2005. Polypeptide models to understand misfolding and amyloidogenesis and their relevance in protein design and therapeutics. *Protein Pept. Lett.* **12:** 171–187.